Grup d'Informació Quàntica >

UAB
Universitat Autònoma de Barcelona

UNIVERSITÉ DE GENÈVE
FACULTÉ DES SCIENCES
Section de physique

Achieving Heisenberg Scaling via interacting many-body dynamics

Ricard Puig i Valls

Thesis submitted for the degree of

Master in Quantum Science and Technology

July 2023

Director: Martí Perarnau-Llobet[1], John Calsamiglia[2]

[1]Quantum Information & Communication, Université de Genève

[2]Quantum Information Group, Universitat Autònoma de Barcelona

This page is intentionally left blank

Thesis submitted for the master's degree of Quantum Science and Technology

Achieving Heisenberg Scaling via interacting many body dynamics

Ricard Puig i Valls

Supervised by: Dr. Martí Peranrnau-Llobet[1], Prof. Dr. John Calsamiglia[2]

[1] Quantum Information & Communication Group, Department of Applied Physics, University of Geneva

[2] Quantum Information Group, Autonomous University of Barcelona

10 July 2023

Abstract

Theoretical models describing quantum metrology schemes and the corresponding experimental demonstrations have so far mainly described step-by-step protocols that involve the preparation of the sensor into a carefully engineered quantum state; interaction of the sensor with an external (unknown) field and measurement of the sensor to retrieve information about the signal. However, the process of preparation can sometimes be lengthy and require fine tuning in time. The main goal of this project is to contribute to this challenge by using many-body interactions to entangle the state while field encodes its information into it. In this way the process of preparing the state is eliminated along with the different challenges that come with it.

Keywords: Fisher Information, Heisenberg Scaling, Magnetometry, Many-body physics, Metrology, Quantum Fisher Information, Quantum Information Theory, Sensing.

Ricard Puig i Valls: ricardpuigvalls@gmail.com

I would like to express my gratitude to the whole Grup d'Informació Quàntica from the Autonomous University of Barcelona and the Quantum Information and Communication group from the University of Geneva for making me fell at home, and specially to both my supervisors, Dr. Martí Perarnau and Prof. Dr. John Calsamiglia. For the academical and personal help. For sharing with me your knowledge, enthusiasm, optimism. For all the help provided during this thesis, and specially for being an inspiration for my science career.

I would also like to thank all my friends and colleagues, new and old, without whom this journey would not have been the same.

Finally, a special thought to my sister and my grandfather. To my sister for being always by my side, and to my grandfather for being the main pillar in my science career. Without you I would not have gotten this far.

Casi tanto como tú

Acronyms

FI	Fisher Information.
GHZ	Greenberger–Horne–Zeilinger.
HS	Heisenberg Scaling.
IID	Independent and Identically Distributed.
MSE	Mean Squared Error.
PDF	Probability Density Function.
POVM	Positive Operator Valued Measure.
QFI	Quantum Fisher Information.
SLD	Symmetric Logarithmic Derivative.
SNL	Shot-Noise Limit.

Symbolist

$\mathcal{F}$	Quantum Fisher Information
F	Fisher Information (Classical)
E	POVM
E_x	Outcome of a POVM
ρ	Density matrix (might be of a pure state)
$\mathbb{1}$	Identity matrix
σ_i	Pauli matrix, $i \in \{x, y, z\}$
$\mathbb{E}[\cdot]$	Expected value
$\mathbb{R}$	Real Number
$\lvert a\rangle \lvert b\rangle$	$\lvert a\rangle \otimes \lvert b\rangle$, Usually the tensor product is not shown.
$\otimes$	Tensor product

Contents

1 Introduction

This thesis delves into the field of Quantum Metrology, with a particular focus on magnetometry, that is, the measurement and estimation of magnetic fields.

Quantum Metrology is an essential field of Quantum Information Theory. It is concerned with the precise estimation of unknown physical parameters, which can range from the strength of a magnetic field to the temperature of ultra-cold gases, by exploiting quantum resources like quantum coherence or entanglement. The precise estimation of physical parameters is of utmost importance in any discipline in natural sciences and has all sort of applications, e.g. medical diagnosis, navigation systems, gravitometry. Thus this has been a widely studied topic [TA14, DDJK15]. Probably the most famous application in recent years of this field is the detection of gravitational waves by LIGO [A$^+$16], however, it has also been used for atomic clocks [LBY$^+$15] or magnetometers [KKAR03].

With the advancement of technology current experiments have managed reduce the noise to a limit where quantum effects are noticeable. The stochastic nature of quantum measurements actually sets a fundamental limit to the estimation precision. Indeed, consider that we have a number of resources N (this can be for example the number of particles or photons, or the duration of the experiment), and we wish to maximise the amount of meaningful information one can obtain on a certain parameter (or any finite number of them) Classically, the only way to improve the precision is to repeat the experiment a number N of times over identically prepared systems thereby reducing the estimation error by a factor $1/N$, the so called Shot-Noise Limit (SNL) or Shot Noise Scaling. However, using quantum mechanical features, notably entanglement, one can find ways to enhance the precision using the same resources by a factor $1/N^2$ (specifically in magnetometry[1]), the so called Heisenberg Scaling (HS) [GLM06, GLM11].

The usual way to proceed when doing quantum metrology is to map the physical unknown quantity to a phase shift in a quantum state. That is, the step by step process involves the preparation of a state used as sensor, the interaction of this state with the signal (i.e. the unknown field), a measurement of the sensor to retrieve information about the signal and a final stage of data analysis optimized to most accurately infer the signal from the measurement outcomes [PSO$^+$18].

However, in the experimental setting, even though there are different examples of overcoming the shot noise limit, either the performance is not close to what could be [WJK$^+$10], or the number of particles used is small [MLS04], thus not taking full advantage of the higher power of the HS. That is because creating and maintaining highly entangled states of large dimension is very difficult[HHR$^+$05] due to the decoherence and noise. Moreover, the preparation of such states, might require long preparation times, and often needs fine tuning in the control interactions.

The main goal of this project is to propose a metrology scheme that might alleviate these problems. For that, this thesis aims to study the possibility of using many-body interactions while the state interacts with the system. This might be able to create entanglement while the system gains information about the unknown parameter, and thereby surpass the SNL.

[1]This can be easily generalized, and will depend on the difference between the maximum and the minimum eigenvalues of the Hamiltonian describing how the external parameter is coupled to the system. In this thesis we will assume that the magnetic field to estimate couples to each system independently ($H = g\sum_i \sigma_{\mathbf{n}}^{(i)}$, where (i) indicates the position of the particle).

2 Metrology formalism

As mentioned above, metrology is the field that studies how and how much information about an unknown parameter can be obtained by a (noisy) measurement. The act of measurement is modeled by taking one or several samples from random variable X whose distribution depends on the unknown parameter, i.e. it is characterized by a family of Probability Density Function's $f_X^\phi(x) = f(x;\phi)$ where x is the measurement outcome and ϕ the unknown parameter. A PDF is defined as

Definition 2.1 (Probability Density Function (PDF))**.** *The PDF $f_X^\phi(x)$ of a random variable X is a non-negative function characterizing the relative likelihood of the possible outcomes of X, or in other words:*

$$\int_{-\infty}^{x} f_X^\phi(x')dx' = Pr(X \leq x;\phi) \ . \tag{1}$$

The family of $\{f_X^\phi(x) : \phi \in \Omega\}$ constitutes the parametric model of the measurement.

With this, the expected value of a function $g(X)$ is defined as:

Definition 2.2 (Expected value)**.** *Given a function $g(X)$, where X is a random variable with a PDF $f_X^\phi(x)$, then the expected value of the function is*

$$\mathbb{E}_X^\phi\left[g(X)\right] = \int_{-\infty}^{\infty} g(x) f_X^\phi(x')dx' \tag{2}$$

In general, both the superscript ϕ and the subscript X will not be written to avoid cluttering of symbols (as long as these are implicit in the context).

If the same experiment is repeated many times under the same conditions, the outcomes will be distributed according to an:

Definition 2.3 (Independent and Identically Distributed (IID))**.** *A collection of random variables $\mathbf{X} = (X_1, X_2, X_3, ..., X_N)$ with a joint PDF $f_{\mathbf{X}}^\phi(x)$ is said to be IID if, given that thePDF's for the random variables X_i are $f_{X_i}^\phi(x)$, then*

$$f_{\mathbf{X}}^\phi(\mathbf{x}) = \prod_i^N f_{X_i}^\phi(x) \tag{3}$$

Under the frequentist approach, the estimated parameter is assumed to be a deterministic variable. For example, if one tries to estimate the phase ϕ in a Bloch vector, it is assumed that this parameter exists, and it is not determined by our measurements[2].

However, this does not mean that this parameter will be ever known. Given a parameter ϕ, the best one can hope for is to possess a reliable estimator for this parameter. This is usually noted like $\hat{\phi}$ and is a statistic, a function of a certain set of outcomes $\mathbf{x}_\phi = (x_1, x_2, ..., x_N)$. Given that the outcomes of a measurement are random variables, our estimator will also be a random variable.

The quality of an estimator is usually quantified by this cost function:

[2]This work will be developed under this assumption. However, it is important to notice that there is also the Bayesian approach. In it, this parameter is itself considered to be a random variable distributed according to a prior PDF.

Definition 2.4 (Mean Squared Error (MSE)). *The Mean Squared Error of an estimator $\hat{\phi}$ for a parameter ϕ is defined as*

$$\mathrm{MSE}\left(\hat{\phi}\right) = \left(\Delta\hat{\phi}\right)^2 = \mathbb{E}_X^{\phi}\left[\left(\hat{\phi}-\phi\right)^2\right] \tag{4}$$

Again, in order to avoid cluttering of symbols in the notation we do not make explicit its dependence on ϕ. However it is important to emphasize that the MSE quantifies the dispersion of the estimated values with respect to the true value, and will generally depend on the value of ϕ.

There are many different estimators. These are chosen according to their simplicity and mathematical properties. A minimal requirement on an estimator is that its value gets closer to the true value as one gathers more measurement data. Mathematically this is characterized by the consistency property.

Definition 2.5 (Consistency). *A sequence of statistics $\{\hat{\phi}_n\}$ is said to be a consistent estimate of a parameter ϕ if for every $\epsilon > 0$*

$$\lim_{n\to\infty} \Pr\left(|\hat{\phi}_n - \phi| \leq \epsilon\right) = 0 \ , \tag{5}$$

for $n \in \mathbb{N}$.

Usually, one also requires this property to hold for all values of the parameter ϕ, at least in a given in interval.

One can define many different estimators that will fulfil this property. A common choice is the parameter that maximizes the Likelihood function. As shown in [MCBS22]

Definition 2.6 (Likelihood Function). *Suppose $\mathbf{X} = (X_1, ..., X_N)$ are jointly continuous random variables whose distribution depends on a parameter ϕ and have a PDF $f(\mathbf{x};\phi)$. The likelihood of the parameter ϕ given $\mathbf{x}$ observations is denoted by $L(\phi|\mathbf{x})$ and is defined to be*

$$L(\phi|\mathbf{x}) := f(\mathbf{x};\phi) \ , \tag{6}$$

From this, one can define the estimator $\hat{\phi}$ such that $L(\phi|\mathbf{x})$ is maximized:

Definition 2.7 (Maximum Likelihood Estimator (MLE)). *Suppose that a sample $\mathbf{x} = (x_1, ..., x_N)$ has likelihood function $L(\phi) = L(\phi|\mathbf{x})$ depending on a parameter ϕ. Then a Maximum Likelihood Estimator (MLE) $\hat{\phi}_{\mathrm{MLE}}$ is the value of the parameter that maximizes $L(\phi)$ if a maximum exists. In other words*

$$\hat{\phi}_{\mathrm{MLE}} = \arg\max_{\phi} L(\phi|\mathbf{x}) \ , \tag{7}$$

This estimator fulfils two important properties. It is consistent[3] and efficient; in other words, it saturates the Cramer – Rao bound [Cra46] in the asymptotic limit of a large number of measurements.

Theorem 2.1 (Cramer-Rao bound). *Let $\mathbf{X} = (X_1, ..., X_N)$ be a jointly continuous random variable with a PDF $f(\mathbf{x};\phi)$, let $\hat{\phi}_N$ be an unbiased estimator of ϕ, such that it does not depend on ϕ for the region with non-zero probability, then*

$$\left(\Delta\hat{\phi}_N\right)^2 \geq F_N^{-1} \ , \tag{8}$$

where F_N is the Fisher Information.

[3]For the interested reader, this property implies that the estimator is unbiased, i.e. $\mathbb{E}\left[\phi - \hat{\phi}\right] = 0$ (however the converse is not true).

Definition 2.8 (Fisher Information (FI))**.** *Let* $\mathbf{X} = (X_1, ..., X_N)$ *be a jointly continuous random variable with a PDF* $f(\mathbf{x}; \phi)$*. Then the FI is given by*

$$F_N := \mathbb{E}\left[\left(\frac{\partial \log L(\phi|\mathbf{x})}{\partial \phi}\right)^2\right] . \tag{9}$$

It is important to notice that due to the additivity property of the FI we can write as $F_N = NF_1$ when $X = (X_1, ..., X_N)$ is a jointly random variable of IID of random variables X_i. This is an important result, as it means that for every measurement the same amount of information is extracted.

Recall that $\hat{\phi}_{\text{MLE}}$ saturates Th. 2.1 in the asymptotic limit. Indeed, this this means that this estimator will extract the maximum information for a given set of random variables $X^N \sim f(\mathbf{x}; \phi)$.

2.1 Quantum Metrology

All these concepts can also be defined for quantum states. In this work, we are mainly concerned with the Quantum Fisher Information. However, let us first introduce some basic definitions and notation. A Positive Operator Valued Measure is, as in [Pre14]:

Definition 2.9 (Positive Operator Valued Measure (POVM))**.** *A POVM* E *is the most general concept of measurement in Quantum Mechanics. It is characterized by a set of operators* $\{E_x\}$ *that have to fulfil the following conditions*

1. *Positivity:* $\langle\psi| E_i |\psi\rangle \geq 0 \; \forall \, |\psi\rangle$ *or in simpler notation* $E_x \geq 0$*.*
2. *Completeness:* $\sum_x E_x = \mathbb{1}$*.*

Now, let ρ_ϕ be a state that depends on the parameter ϕ. If we choose POVM E with outcomes E_x and make a measurement into the state, the outcome of such measurement will be a random variable X distributed according to a PDF $f_X^\phi(x) = \text{Tr}\{E_x \rho_\phi\}$. With this probability distribution, we can compute the FI. This is, according to Def. 2.8

$$F = \sum_x \frac{\text{Tr}\{E_x \partial_\phi \rho_\phi\}^2}{\text{Tr}\{E_x \rho_\phi\}} . \tag{10}$$

However, as there are infinitely different POVM's to choose, and each of them might give a different PDF, it is not automatic which one to choose. Luckily, this can be avoided via the Quantum Fisher Information.

Definition 2.10 (Quantum Fisher Information (QFI))**.** *Let* ρ_ϕ *be a state and* E *a POVM, then the QFI is defined as follows*

$$\mathcal{F} = \max_E F(\rho_\phi, E) . \tag{11}$$

This can be written in terms of a closed formula [BC94a], depending only on $\rho_\phi = \sum_k \lambda_k |k\rangle\langle k|$ *and its derivative* $\partial_\phi \rho_\phi$ *with respect to the unknown parameter:*

$$\mathcal{F}(\rho_\phi) = 2 \sum_{k,l} \frac{|\langle k| \partial_\phi \rho_\phi |l\rangle|^2}{\lambda_k + \lambda_l} . \tag{12}$$

Another way of defining the QFI is via the Symmetric Logarithmic Derivative. This is

Definition 2.11 (Symmetric Logarithmic Derivative (SLD))**.** *The Symmetric Logarithmic Derivative (SLD) is denoted as L_ϕ is defined in the following way. For a state ρ_ϕ that depends on a parameter ϕ*

$$\frac{L_\phi \rho_\phi + \rho_\phi L_\phi}{2} = \partial_\phi \rho_\phi \ . \tag{13}$$

With this definition, the QFI can be written as

$$\mathcal{F}(\phi) = \mathrm{Tr}\Big\{L_\phi^2 \rho_\phi\Big\} \ . \tag{14}$$

Now, if $\rho_\phi = |\rho_\phi\rangle\langle\rho_\phi|$ is a pure state[4], the QFI can be rewritten as

$$\mathcal{F}(\rho_\phi) = 4(\langle\partial_\phi\rho_\phi|\partial_\phi\rho_\phi\rangle - |\langle\partial_\phi\rho_\phi|\rho_\phi\rangle|^2) \ . \tag{15}$$

When considering ρ_ϕ a pure state, the dependance on ϕ can be written as $\rho_\phi = e^{-iA_\phi}|\rho_0\rangle\langle\rho_0|e^{iA_\phi}$ where A_ϕ is an Hermitian matrix that depends on ϕ. Now, particularly, in the case of $A_\phi = \phi t H$, the QFI can be written as

$$\mathcal{F} = 4t^2(\Delta H)^2_{\rho_0} \ , \tag{16}$$

i.e. the variance of H with respect to the initial state.

The above expression for the QFI gives the optimal (classical) FI extracted via a E measurement. However, it is often important to construct the POVM that attains it. Any POVM $E = \{E_x\}$ attaining the QFI must satisfy the following conditions

- $\mathrm{Tr}\{E_x\rho_\phi L_\phi\} \in \mathbb{R}$
- For every outcome of the POVM E_x, a $c_x \in \mathbb{R}$ exist such that

$$\sqrt{E_x}\sqrt{\rho_\phi} = c_x\sqrt{E_x}L_\phi\sqrt{\rho_\phi} \ . \tag{17}$$

There is also a quantum counterpart to the Th. 2.1. This is the Quantum Cramer-Rao bound [BC94b], and states that the bound on the variance imposed by the QFI is also attainable asymptotically with the number of measurements.

Now that all the mathematical tools required are defined, let us start with the problem to study.

[4]For pure states $|\rho\rangle$ is understood to be the unique nonzero eigenstate of ρ. That is $\rho = |\rho\rangle\langle\rho|$.

3 Magnetometry

Magnetometry is defined as the study of the measurements of magnetic fields. When someone wants to measure the strength of a magnetic field, i.e. estimate the parameter g from the following Hamiltonian $H = gS_z$, the usual (classical) approach will consist of the following three steps, as can be seen in Fig. 1:

a) Take a spin particle perpendicular to the direction of the magnetic field in the Bloch Sphere (so the state feels the maximum amount of "change").

b) Let the spin particle evolve under the magnetic field S_z, for a known time t.

c) Measure the final state to retrieve information from the magnetic field.

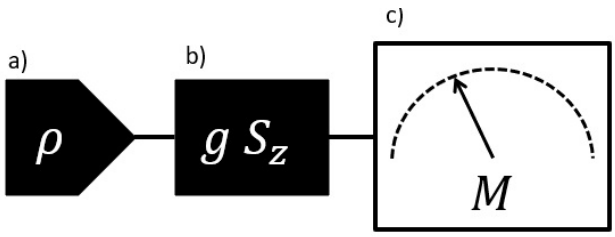

Figure 1: **Canonical quantum metrology scheme:** (a) Take a spin particle ρ perpendicular to the direction of the magnetic field. (b) Let it evolve a time t, (c) Make a measurement M on the particle.

To get an estimator $\hat{g}$ for the parameter g, the procedure is repeated independently N times or, equivalently, the quantum system consists of N independent spins, i.e. its state does not exhibit quantum correlations. Since this corresponds to the IID sampling presented above it inevitably leads to a MSE with SNL, i.e. as $1/N$. Even doing more sophisticated collective measurements cannot improve this since the QFI is additive. That is, for IID states $\mathcal{F}(\rho_g^{\otimes N}) = N\mathcal{F}(\rho_g) = t^2N$, where we have used (16) to compute the single particle QFI, $\mathcal{F}(\rho_g) = 4t^2(\Delta H)^2_\rho = t^2$. Using this procedure, the advantages that the quantum realm can provide to us are not taken into account, and the QFI scales as $\mathcal{F} = t^2N$. That is, to reduce the variance of your estimator to $\frac{1}{N}$, N resources will be required.

However, the quantum realm, and especially taking advantage of entanglement, allows for much faster convergence. That is if one entangles the initial state in some particular way[5], less than N resources will be required to reduce the variance of your estimator by a factor $1/N$. In order to exploit the quantum correlations, one can adapt the previous protocol in the following way (see also Fig. 2).

a) Take N spin particles[6].

b) Entangle these particles into a state that will give you an advantage with respect to the SNL.

c) Let the entangled state evolve under the magnetic field S_z, for a known time t.

[5]The entanglement must be done in such a way that allows for a higher QFI. Some examples can be found in [TA14]. Moreover, for the interested reader, the role of entanglement in Quantum Metrology has been studied asymptotically here [AKS+16].

[6]Given that some unitary operations will be applied to these particles, there is no need to require any other restriction.

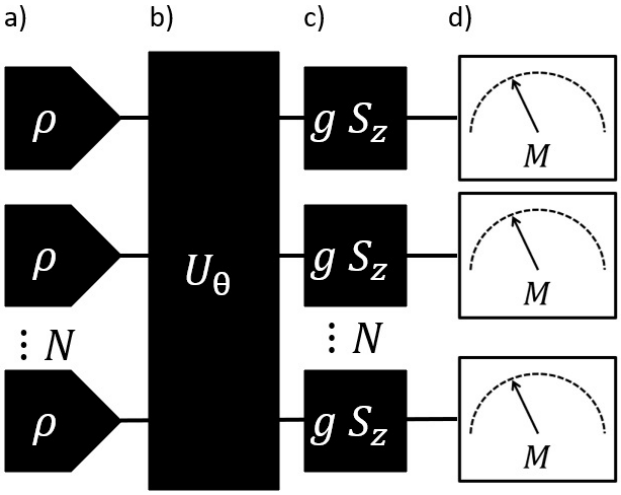

Figure 2: **Scheme to obtain Heisenberg Scaling ($\mathcal{F} \propto N^2$):** (a) Take N spin particles. (b) Entangle them. (c) Let the entangled state evolve a time t under the magnetic field, (d) Make a measurement M on each particle.

d) Measure the final state to retrieve information from the magnetic field. Of particular relevance are those measurements which are local, that is one can measure each particle separately.

The most efficient state to do so is the so-called Greenberger–Horne–Zeilinger (GHZ) state [GHSZ90]. Defined as

$$|GHZ\rangle = \frac{1}{\sqrt{2}}\left(|\lambda_{\max}\rangle^{\otimes N} + |\lambda_{\min}\rangle^{\otimes N}\right) , \tag{18}$$

where $|\lambda_{\max,\min}\rangle$, refer to the states which have larger and lower eigenvalues of the magnetic field, i.e. $gSz\,|\lambda_{\max,\min}\rangle = \pm g\frac{N}{2}\,|\lambda_{\max,\min}\rangle$[7]. That is because this state is the one that maximizes the variance of S_z, as $\langle S_z\rangle_{GHZ} = 0$, and $\langle S_z^2\rangle_{GHZ} = ||S_z^2||$.[8]. The QFI is $\mathcal{F} = t^2N^2$. This is referred to as Heisenberg Scaling (HS), and it reduces the number of resources required by one order of magnitude.

Other quantum states can give a $\mathcal{F} = \gamma N^2 t^2$ where $\gamma \in (0, 1]$. These states are very variate, but they all share one characteristic: they are highly entangled states that minimize the expected value of S_z while taking advantage of the quantum correlations to maximize the expected value of S_z^2. Here we put a lot of emphasis on the QFI being of the order $\mathcal{F} \sim t^2N^2$, however, it is important to highlight that anything above $\mathcal{F} = t^2N$ is a quantum advantage.

As mentioned in the introduction, the practical implementation of such schemes is far form this ideal situation. The difficulty to prepare the GHZ state, the presence of noise and limited experiment duration makes it hard to reach a practical quantum advantage in sensing. With the hope to solve (at least partially) some of these problems, in this work we will put forward an approach that breaks with the standard paradigm presented above.

[7]For a magnetic field, i.e. a set of spins, the $|GHZ\rangle = \frac{1}{\sqrt{2}}\left(|0\rangle^{\otimes N} + |1\rangle^{\otimes N}\right)$, where $|0\rangle$, $|1\rangle$ are the eigenstates of σ_z. It is usually referred to as the maximally entangled state.

[8]Here $||\cdot||^2$ stands for the operator norm defined as $\max_\phi \langle\cdot\rangle_\phi$.

4 Dynamical Fisher Information with no entanglement

In this thesis, we will use many-body controlled interactions that will generate entanglement while at the same time encoding the information of g into the state. Therefore, the Hamiltonian that will determine the evolution of the state is

$$H = gS_z + \sum_j \lambda_j h_j \ , \tag{19}$$

where the $\{\lambda_j\}$ are control parameters and $\{h_j\}$ are the associated operators. This can potentially reduce the overall time of the protocol (hence reducing decoherence/dissipation) and avoids using time-dependent control. More precisely, the approach presented is the following

1. Prepare a product state, i.e. a pure state with no quantum correlations.
2. Let the estate evolve under the Hamiltonian in Eq. (19). This substitutes steps (b) and (c) in the previous protocol (Fig. 2).
3. Measure the final state to retrieve information from the magnetic field. This measurement can in principle be arbitrary, although one can considers schemes with some restrictions (e.g local, repeated, separable).

Fig. 3 shows a comparison between the two approaches. In this new approach the two-step process of entangling and encoding the information into the state (via a phase difference) is done at the same time. Moreover, while the previous approach (Fig. 3a) requires some form of time-dependent control to prepare the state, in this one (Fig. 3b) this is not required. This is because the interaction is switched on and kept. This protocol might also be more resistant to noise and decoherence[9].

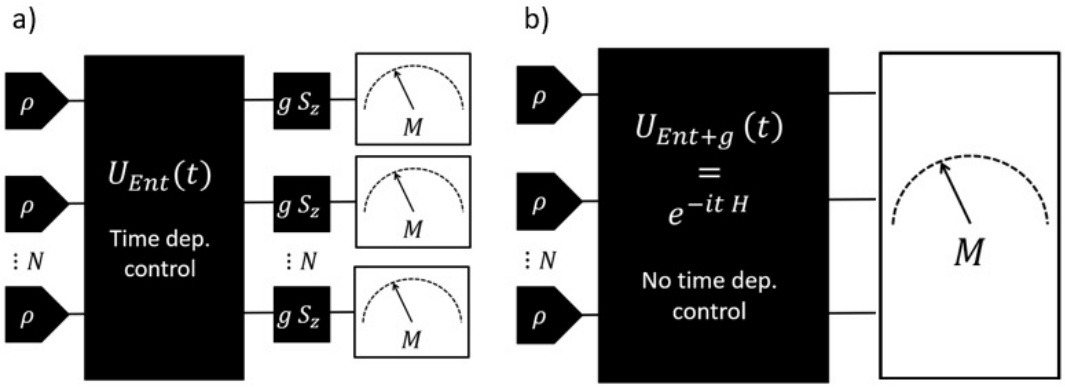

Figure 3: Comparison between a) the standard approach explained in the previous section and b) the new approach studied here, consisting on entangling the state and embedding the parameter g to it at the same time.

In this setting it is not clear how the QFI will behave, or even whether HS will be achievable. Given that we will use pure states, the starting point will be the expression of the QFI given in Eq. (15). The initial state is taken to be an uncorrelated (product) pure

[9] Intuitively, this is justified because the interaction is kept on during the estimation process. Then when the state decays or suffers from noise, it will be prepared "again" into an entangled state.

state denoted by $|\rho_0\rangle$, and it evolves under $U(t) = e^{itH(g)}$, where H is the Hamiltonian from Eq. (19) and g is the unknonw parameter. Then using the derivation by [Wil67]

$$|\dot{\rho}_g\rangle := \frac{d}{dg}U|\rho_0\rangle = -it\int_0^1 e^{-istH}S_z e^{-i(1-s)tH}ds\,|\rho_0\rangle \ . \tag{20}$$

With this expression, one can show that for the long-time regime, we get a very similar expression to Eq. (16). Let P_k be the projectors of the Hamiltonian in Eq. (19), that is $H = \sum_k E_k P_k$. Then if we define the Pinched Hamiltonian as $H_p = \sum_k P_k S_z P_k$, the QFI is

$$\mathcal{F} \approx 4t^2(\Delta H_p)^2_{|\rho_0\rangle} \ . \tag{21}$$

Sketch of the proof[10]
To see this one just needs to realize that when expressing Eq. (20) in its projector form, the only terms that will be proportional to t are those in which the product of the exponential eigenvalues equals one, that is

$$\int_0^1 e^{-istH}S_z e^{istH}ds = \int_0^1 \sum_{j,k}^{N} e^{-ist(E_k-E_j)}P_k S_z P_j ds = \sum_k P_k S_z P_k + \frac{1}{t}\sum_{k,l|k\neq l} P_k S_z P_l c_{k,l} \tag{22}$$

where $c_{k,l} = \frac{e^{-itE_k}-e^{-itE_j}}{E_k-E_j}$ are bounded. This can be readily understood, since for times much larger than the smallest energy gap in the Hamiltonian, the rapid oscillating phase in the integral will cancel, except when $k = j$.

Notice this expression gives us some insights into the properties of our choice of Hamiltonian to surpass the SNL. Mainly, for the long-time regime, one sees that the entanglement is being shifted from the states as in Fig. 3a, to the eigenstates of S_z, the magnetic field in Fig. 3b using the "pinching" (i.e. the action of erasing out diagonal blocs, $\sum_k P_k S_z P_k$).

However, this result does not assure us in any way that HS can be achieved. To show it, a protocol that achieves it is presented.

[10] Find a full proof at Annex A.

5 Protocol 1: Many Body

With this protocol, the maximum QFI that one can achieve is $\mathcal{F} = \frac{1}{2}N^2t^2$. Thus, HS is achievable. This protocol consists of the following. Consider the Hamiltonian in Eq. (19), then the terms $\{\lambda_j h_j\}$ are defined as follows

$$\sum_j \lambda_j h_j = N\lambda \left(|N\rangle\langle 0| + |0\rangle\langle N| + |-N\rangle\langle 0| + |0\rangle\langle -N|\right), \tag{23}$$

where $S_z |\pm N\rangle = \pm\frac{N}{2}|N\rangle$ are the states with all N spins up or down respectively, while $S_z|0\rangle = 0$ is a state with the same number of spins up than spin downs. Note that the zero eigenspace of S_z is very degenerate, so this choice of $|0\rangle$ is not unique. However, since the optimal input state is also $|\rho_0\rangle = |0\rangle$, if this ought to be a product state we must choose $|0\rangle := |\uparrow\rangle^{\otimes\frac{N}{2}} |\downarrow\rangle^{\otimes\frac{N}{2}}$ or permutations thereof.

With this, the QFI is dependant on the relation between g, λ,

$$\mathcal{F} = 4t^2N^2\frac{g^2\lambda^2}{(g^2+2\lambda^2)^2}\ . \tag{24}$$

As said before, the maximum of $f(g,\lambda) = 4\frac{g^2\lambda^2}{(g^2+2\lambda^2)^2}$ has a maximum at $\frac{1}{2}$. That happens when $\lambda = \frac{g}{\sqrt{2}}$, as can be seen in Fig. 4.

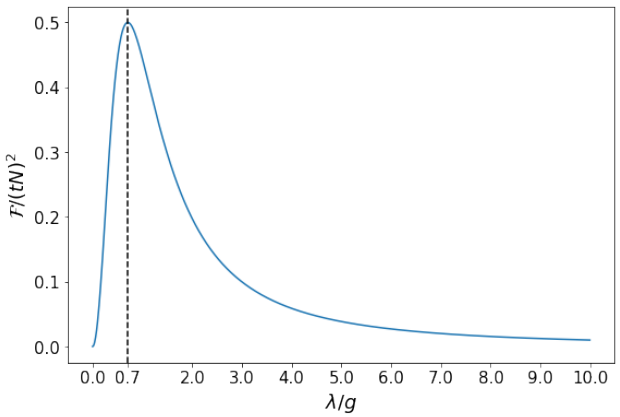

Figure 4: Representation of the QFI normalized with the factor N^2t^2 with respect to λ/g. In this figure one can appreciate that when λ is close to $g\frac{1}{\sqrt{2}}$ the QFI $\mathcal{F} \to \frac{1}{2}N^2t^2$.

Sketch of the proof[11]
The intuition behind this result is connecting the highest and lowest values of our Hamiltonian, basically doing the same as the GHZ state does. Follows easily from writing the interacting Hamiltonian as

$$\sum_j \lambda_j h_j = N\lambda\sqrt{2}\left(|GHZ\rangle\langle 0| + |0\rangle\langle GHZ|\right)\ , \tag{25}$$

where $|GHZ\rangle$ is the one in Eq. (18). As an intuition, the prefactor of $\frac{1}{2}$ of the $\mathcal{F}$ can be seen as being one half of the time in the $|GHZ\rangle$ and the other in the $|0\rangle$ state.

Even though it might be counter-intuitive that the QFI depends on the parameter that we are trying to estimate, it is not something uncommon. However, this might indeed

[11] Find a full proof at Annex B.

cause some problems when trying to estimate the parameter. One can use other methods using few resources to get a rough estimate of g, and then use this strategy to reduce it to HS[12].

Overall, here it is shown that this way of proceeding can lead to HS. That is, the best quantum advantage when doing magnetometry can be achieved, even when g is very small.

5.1 Comparison with the standard GHZ state protocol

Let us highlight the two main difference between the our scheme (Fig. 3b with the interacting term in Eq. (23)) and the protocol using a GHZ (Fig. 3a using the state shown in Eq. (18)):

1. **Preparation:** The standard protocol, requires a preparation stage. In particular to attain the optimal scaling one needs to prepare a GHZ state , for example by applying consecutive CNOT gates to the state $|+\rangle |0\rangle^{\otimes N}$. This means that the unitary operation
$$U_{i,i+1}(\tau) = e^{i\tau(\mathbb{1}^{(i)} - \sigma_z^{(i)}) \otimes (\mathbb{1}^{(i+1)} - \sigma_x^{(i+1)})} \tag{26}$$
with a precise time of $\tau = \pi/4$ has to be applied in every pair of particles (indicated by the labels $i, i+1$). Thus fine time tuning is required.

   In the strategy studied in this thesis (Fig. 3b), there is no preparation. Therefore, no time tuning is required.

   A challenge of our protocol is that it requires N-body interactions, whereas the standard one can be done concatenating two-body operations (CNOT gates). This motivates next section. Also the preparation of the GHZ will increase linearly with N, dis does not happen for the protocol studied here.

2. **Scaling:** In the standard protocol to achieve HS (Fig. 3a) the QFI scales as $\mathcal{F} = N^2 t'^2$. t' is the time that one lets the state interact with the Hamiltonian (step c of Fig. 2).

   In the strategy studied in this thesis (Fig. 3b), the QFI is $\mathcal{F} = \frac{1}{2} N^2 t^2$ (in the best case scenario). However, because there is no preparation of the state, this time compared to the protocol with the GHZ is $t = t' + \tau$. Basically, this means that by avoiding the preparation step, more time is put into the encoding, thus a higher scaling is achieved.

Here it is shown that both protocols are different in nature, therefore they lead to different results and also have different requirements to give the maximum scaling. Last but not least, let us point out that the proposed scheme serves the purpose to show that quantum correlations, required for HS, can be established while the sensor is exposed to the magnetic field. However, the required Hamiltonian in (23) is not readily available in nature, and it seems very unlikely that it can be engineered. With this in mind next section is devoted to find more feasible schemes requiring only two-body interactions.

[12] A possible approach might be to use the Standard Quantum Limit get an estimate of g to bound the function $f(g, \lambda)$ and then use this protocol.

6 Protocol 2: Two Body

Motivated by the possibility of implementing this approach experimentally, now we consider two-body interactions. These interactions have a Hamiltonian of the following form

$$H = \sum_{i,j} c_{i,j,k,l} \sigma_k^{(i)} \otimes \sigma_l^{(j)} \ , \tag{27}$$

where $\sigma_k \in \{\mathbb{1}, \sigma_x, \sigma_y, \sigma_z\}$, for $k \in \{0, x, y, z\}$ and where the (i) in $\sigma^{(i)}$ indicates the position of the particle in the chain (or surface, 3d-space, etcetera).

6.1 Quantum advantage using one-axis twisting Hamiltonian

Now, we show that we can achieve a quantum advantage using just a one-axis twisting control term, i.e. $S_x^2 = \sum_{i,j}^N \sigma_x^{(i)} \otimes \sigma_x^{(j)}$ (where the indices i, j refer to the position of the particle), that is, all the particles interact with each other with the same weight[13]. Notice that this interaction, where there is an all-to-all Hamiltonian (as in Eq. (27)) and the number of particles is very high, might be very difficult to implement in systems based on localized qubits (such as those in a quantum computer), but is very natural in atomic ensembles used in magnetometry.

The proof for the quantum advantage turns out to be quite subtle. Let us consider $H = gS_z + \lambda S_x^2$ and a state with an $N-$odd number of particles. Then if $\lambda \gg g$, it can be proven that

$$\mathcal{F} = t^2 \frac{N^{3/2}}{\sqrt{2\pi}} + \mathcal{O}\left(\frac{g}{\lambda}\right) . \tag{28}$$

That is, by letting N particles (where N is odd), pointing initially in the y direction in the Block Sphere[14], and letting them evolve under this Hamiltonian with the controlled parameter λS_x^2, one can get over the Shot Noise Limit by a factor of $\sqrt{N}$.

Scketch of the proof[15]
First notice, that in the eigenstates of S_x^2, S_z will act as a linear combination of the ladder operators S_+, S_-. That is

$$S_z \left|s_x, m\right\rangle \propto a \left|s_x, m+1\right\rangle + b \left|s_x, m-1\right\rangle \ , \tag{29}$$

where a, b are the constants given by the ladder operators S_+, S_-.
$\left|E_k\right\rangle = \left|E_k\right\rangle^{(0)} + \frac{g}{\lambda}\left|E_k\right\rangle^{(1)} + \mathcal{O}\left(\frac{g^2}{\lambda^2}\right)$, where (i) refers to the order of the correction[16]*. By imposing large times one can compute $\mathcal{F}$ via Eq. (21).*

When computing the pinched Hamiltonian H_p, since S_z will again behave as a linear combination of ladder operators, the only "pinching" that will survive at $0-$th order will

[13] The operators S_x, S_y, S_z refer to the generalized spin. More information can be found in [SN13]. This operators are defined as $S_{\mathbf{n}} = \sum_{i=0}^N \sigma_{\mathbf{n}}^{(i)}$, where $\mathbf{n}$ represents the direction of the Pauli Matrices. Therefore, these are one-body interactions and $S_{\mathbf{n}}^2$ are two-body interactions.

[14] For the unfamiliar reader, the Block Sphere is the geometrical representation of the space of one qubit. For more information please review the section *Quantum Bits* from [NC10].

[15] Find a full proof at Annex C.

[16] The $0-$th order eigenstate will be also affected by the perturbation as S_x^2 is degenerate. Thus the perturbation breaks this degeneracy.

be the subspace of $m_x = \pm\frac{1}{2}$ *(e.g.* $\left\langle s_x, m = \frac{5}{2}\right| S_z \left|s_x, m = \pm\frac{5}{2}\right\rangle = 0$*). This is why the condition of an* $N-$*odd number of particles is required.* H_p *then looks like*

$$H_p = \sqrt{\frac{N}{2}\left(\frac{N}{2}+1\right) - \frac{1}{4}}\left(|s_x,+\rangle\langle s_x,+| - |s_x,-\rangle\langle s_x,-|\right) \ , \tag{30}$$

where

$$|s_x,\pm\rangle = \frac{1}{\sqrt{2}}\left(\left|s_x, m = \frac{1}{2}\right\rangle \pm \left|s_x, m = \frac{-1}{2}\right\rangle\right) + \mathcal{O}\left(\frac{g}{\lambda}\right) \ . \tag{31}$$

Finally, it is just a problem of optimization to see which state of the form of $|\theta,\phi\rangle^{\otimes N}$ *maximizes the QFI. Intuitively, the state of that will maximize this is in the* y *direction because it will "feel" both interactions the most. And it is. Therefore, the state that is chosen is* $|y\rangle^{\otimes N}$*, to finally obtain Eq. (28).*[17]

Now that we have shown there is a quantum advantage, we study how robust these results are, i.e. how far can the setting be from the assumptions to work. Firstly, in Fig. 5a it is clear that the time convergence to the QFI given by Eq. (21) is very fast with just one unit of time (in natural units) the value already reaches the "steady state". Moreover, both N and g/λ do not affect such convergence in a significant way[18]. The convergence of this protocol to the "steady state" seems independent of the relation g/λ (as long as it is small). That is, for a fixed N the QFI does not vary when changing g/λ. Regarding the value of N, it might seem that lower values of N converge faster to this value. However, as can be seen in Fig. 5b the lower values of N have a higher value of $\mathcal{F}/(t^2N^{3/2})$. Therefore, it is just a matter on where the "steady state" is.

This brings us to Fig. 5b, where the relation between N and $\mathcal{F}/(t^2N^{3/2})$ is shown. Clearly, for all values of g/λ the smaller N the higher $\mathcal{F}/(t^2N^{3/2})$. Also, the approximation breaks down for values of $g/\lambda \gtrsim 0.001$. This is because in this setting the terms $\mathcal{O}(g/\lambda)$ start having a significant weight due to the correction of S_z being more significant.

The last figure in this set of plots is Fig. 5c). The relation between $\mathcal{F}/(t^2N^{3/2})$ and g/λ is shown for a different number of particles. The important, or most interesting aspect of this figure is how, for the larger values of N the approximation breaks down.

6.2 Comparison with one-axis twisting using the standard protocol.

Let us compare this protocol to the standard scheme in Fig. 3a. There are several papers [PS09] studying the effects of a non linear evolution of $S_{\mathbf{n}}^2$ to prepare the state (that is, using $U = e^{-i\tau S_{\mathbf{n}}^2}$ in step b of Fig. 2) to do magnetometry. The two main differences are outlined next and summarized in Table 1:

1. **Preparation:** As mentioned before, both protocols use the same interaction term. The protocol presented in [PS09] (of the type of Fig. 3a) requires the previous preparation of the state. This time is independent of the dimension of the state. Whereas the protocol studied in this thesis (Fig. 3b) does not require any preparation time. However, the protocol studied in this thesis requires and odd number of particles N.

2. **Scaling:** The protocol studied in [PS09] (of the type of Fig. 3a) achieves a QFI of $\mathcal{F} \sim t'^2N^2f(\tau)+\mathcal{O}(N)$, where τ is the preparation time. $f(\tau) \in [0,1]$ is bounded and dependant on τ. Therefore a small change in the preparation time can change the

[17] Notice that there might be a state that gives a further advantage in this protocol. However, we have restricted ourselves to the set of states $|\theta,\phi\rangle^{\otimes N}$

[18] Recall that the QFI is natural such that $\mathcal{F}/(t^2N^{3/2})$

prefactor in the QFI[19]. Also, notice that t' is the time in which the state is interacting with the field to study (step c of Fig. 2). For the protocol studied in this thesis (of the type Fig. 3b), the QFI behaves as $\mathcal{F} \sim t^2 N^{3/2}$ and it works only for $N-$odd number of particles. Therefore, the two main differences are the power in the scaling with the dimension ($N^2 f(\tau)$ vs $N^{3/2}$) and the scaling with time (t'^2 vs $t^2 \sim (t'+\tau)^2$).

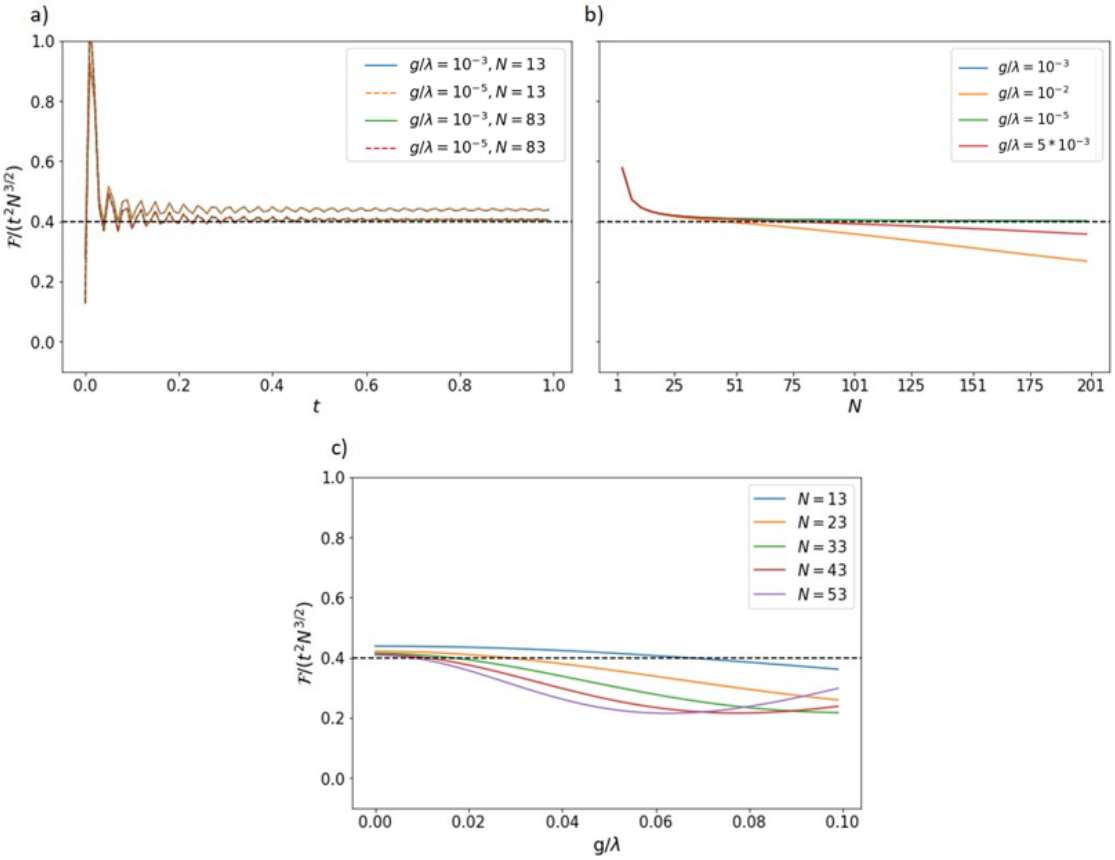

Figure 5: Representation of the different relations of $\mathcal{F}/(t^2N^{3/2})$ with parameters of the problem. The dashed line represents the QFI from Eq. (28). (a) Relation of $\mathcal{F}/(t^2N^{3/2})$ with t (in natural units) for two radically different values of $\frac{g}{\lambda}$ and N. It can be seen that the effects of $\frac{g}{\lambda}$ are null in the convergence to the H_p expression. However, there is a small effect due to N. (b) Relation between the $\mathcal{F}/(t^2N^{3/2})$ and the number of particles used (recall that N is always odd) for different relations between g/λ. Here it is very clear that the approximation holds up to $g/\lambda = 0.001$. (c) Relation between $\mathcal{F}/(t^2N^{3/2})$ and g/λ (at the long time regime) for a different number of particles used. This figure highlights the fact that the higher the number of particles, the smaller the relation between g/λ has to be.

[19]Notice that $f(\tau)$ can also have a value of 0 in extreme cases. This means the quantum advantage of the protocol can be completely destroyed.

Table 1: Comparison between the the standard approach shown in Fig. 3a and the approach studied in this thesis (Fig. 3b). Both for using the non-linear interaction $S_{\mathbf{n}}^2$.

	Standard approach	**Approach studied here**
Requires preparation	Yes	No
Requires fine time tuning (τ)	Yes	No
Scaling in time ($\mathcal{F}$)	$t' \sim (t-\tau)^2$	t^2
Scaling in the dimension (N)	N^2	$N^{3/2}$
Dependency on the parity of N	No	Yes

6.3 Achieving QFI with local observables.

Finally, we will show that, quite crucially, our bounds can be attained by a simple, experimentally available measurement. We show that measuring the observable S_x is enough. To prove so, compute the FI[20] F of the state $\rho = U\left|y\right\rangle\!\left\langle y\right|^{\otimes N} U^\dagger$, where U gives the evolution under $H = \lambda S_x^2 + gS_z$. With this measurement $F_{S_x} = \mathcal{F}$.

Scketch of the proof[21]
This proof is long but very simple to see. Just notice that the projectors E_i into the subspace of $|s_x, \pm\rangle$ (i.e. the subspace of H_p) for $E = S_x$ are into the states $\left|s_x, \frac{\pm 1}{2}\right\rangle$. Then substitute this into Eq. (10) and you find $F_{S_x} = \mathcal{F}$. One would also expect this observable to be, as is the one that will be able to measure the most change from S_z without being affected by the one-axis twisting caused by S_x^2.

The fact that this can be achieved with macroscopic measurements is of the most importance. That is because the whole idea of this project is to avoid applying intricate operations, usually very difficult to perform in an experimental setting, However, if the measurements were to be non-macroscopic and entangled, that would just seem like shifting the intricacies, from the beginning of the protocol to the end. Nevertheless, let us note that this is still a nontrivial interesting task because performing intricate POVM's is often easier than preparing nontrivial states.

In addition, note that while entanglement is strictly necessary to achieve HS, as pointed out in [GLM11], the QFI can be always achieved using the asymptotic limit of large N, with an estimation strategy constructed via local measurements and adaptive estimators, a strategy that employs only Local Operations and Classical Communication (LOCC). And even though this might seem to solve the problem, finding the adaptive estimators might be extremely complicated.

In this section, it has been shown that a quantum advantage (even though not full HS) is possible using the approach in Fig. 3b) with only two-body interacting terms. Thus making it more feasible to produce in an experimental environment. Finally, it has been proven that this can be achieved by performing macroscopic (local) measurements that do not require to adress individual particles. This final point, also being of out-most importance due to the feasibility of implementing such measurements.

[20] For the experienced reader, you might be wondering why the Error Propagation Formula, $(\Delta g)^2 = \frac{(\Delta E)^2}{\left|\partial_g \langle E\rangle\right|^2}$, is not used. As highlighted in [PSO+18] this is just an approximation and is not always valid.

[21] Find a full proof at Annex D.

6.4 Improving the quantum advantage in the symmetric space

Using *Pytorch* [PGM+19] a library for *Python*, we have been able to show numerically that there are protocols that perform even better. More specifically, we have used the Adam[22] process for stochastic optimization to perform a gradient-based optimization on the QFI. These gradients are computed using automatic differentiation[23], to ensure a better convergence and precision for the QFI. Using these tools we optimize over a larger family of symmetric Hamiltonians and show that better scaling for the QFI can be attained. These results are as follows. Firstly, the states that are chosen are [MWSN11]

$$|\eta\rangle = |\theta_z, \phi_z\rangle^{\otimes N} = \frac{1}{(1+|\eta|^2)^s} \sum_{m=-s}^{s} \binom{2s}{s+m}^{1/2} \eta^{s+m} |s_z, m\rangle \ , \tag{32}$$

where $\eta = -\tan\left(\frac{\theta}{2}\right) e^{-i\phi}$. This is because to achieve HS one usually takes advantage of the symmetric space (where S^2 has a maximum value). Moreover, the dimension of the symmetric space grows linearly with the number of particles ($\dim_{\text{sim}} = N+1$ vs $\dim_{\text{tot}} = 2^N$ for all the space). With this the QFI can be modelled for a larger number of particles, therefore the asymptotic limit for N (when the number of particles N is large) can be studied.

Motivated by these considerations, we define the Hamiltonian as $H = gS_z + \alpha S_x^2 + \beta S_y^2$, where g is the unknown magnitude. Therefore we optimize over 4 parameters. $\{\theta, \phi, \alpha, \beta\}$.[24] Furthermore, the optimization will be conducted for the long-time regime. That is, mathematically one could set it into Eq. (21).

With this optimization we find that the following Hamiltonian $H' = gS_z + \lambda S_x^2 + \frac{1}{\sqrt{N}} S_y^2$ achieves a higher scaling than the protocol we showed before, for $g \ll \lambda$. The full list of parameters is $\{\theta = \frac{\pi}{4}, \phi = \frac{\pi}{2}, \alpha = \lambda, \beta = \frac{1}{\sqrt{N}}\}$ [25]. In Fig. 6 different results for this optimization are shown.

First of all, it is important to realize that the same condition in N for long-time regimes holds. The plot is done for $N-$odd number of particles. Because for N even, the results of the optimization are once again 0. This comes, again, from the "pinching" as when having S_z act as a ladder operator, only certain sub-spaces survive.

In Fig. 6, it is apparent there is a significant increase in the value of the $\mathcal{F}/(t^2 N^{3/2})$, in relation to N. This protocol seems to outperform the one shown before, and not by a constant, but by a value dependant on N. This clearly suggests the possibility of a different scaling in N. That is, almost all the combinations shown, the QFI is higher and dependant on N. This motivates us to look for another normalization. This is shown in Fig. 7. Here we change the normalization constant from $\mathcal{F}/(t^2 N^{3/2})$ to $\mathcal{F}/(t^2 N^2)$.

In Fig. 7a the relation between $\mathcal{F}/(t^2 N^2)$ and t (in natural units) is presented. It is seen that in this protocol the convergence to the "steady state" is very similar to the previous protocol. The effects of N and g/λ are negligent in reaching such steady state.

[22] This is one type of algorithm to compute stochastic optimizations of functions using first-order gradient descent. A process that takes advantage of the local derivatives to "search" for the minimum of a function. More information can be found here [KB17]

[23] This is a process that combines analytical derivatives and the chain rule ($\partial_x f(g(x)) = f'(g(x)) * g'(x)$) with numerical differentiation to make the computation of the gradients both more efficient and precise.

[24] Find the full code for the optimization in Annex E

[25] The parameter λ has to fulfil the condition of $g \ll \lambda$. However, for consistency, it has been chosen at $\lambda = 100$. This condition is imposed so the results are somewhat independent of the other variables. Otherwise, the behaviour of the QFI is extremely sensitive to the dimension and g. Also for each g, N the landscape of optimization is very flat, thus it takes a lot of resources to optimize the values.

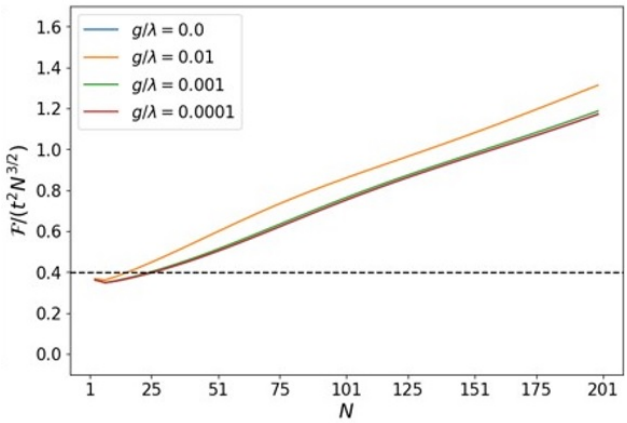

Figure 6: Relation between the $\mathcal{F}/(t^2N^{3/2})$ and the number of particles used (recall that N is always odd) for different relations between g/λ, and for the long time regime. Here it is very clear that even when $g = 0$, the current protocol outperforms Eq. (28). In this setting, when $g/\lambda < 0.001$ the changes are insignificant. However, when g/λ is increased this changes.

Fig. 7b reflects the main purpose of the re-scaling. It is seen that independently of the values of g/λ (for the regime of large times) there is HS. In this figure, we also plot two different regressions of the type $f(N) = a+b/\sqrt{N}+c/N$ for $g/\lambda = 0$, $g/\lambda = 0.01$, shown in dotted lines. This are, respectively $f_{g=0}(N) = 0.141-1.193/\sqrt{N}+5.498/N$, $f_{g=10^{-2}}(N) = 0.196 - 2.311/\sqrt{N} + 12.159/N$. Also, we plot the asymptotic limit of this functions shown in dashed lines. Both of them are shown to converge to HS. Therefore, we expect that if this results are extended to a dimension as high as desired, the value of $\mathcal{F}/(N^2t^2)$ would converge to this one shown by the dashed lines. That is, we expect to achieve a $\mathcal{F} \approx 0.15t^2N^2$ in the asymptotic limit.

Lastly, Fig. 7c shows that in the regime of $g/\lambda \ll 1$ larger values of this relation increase the QFI. This is not independent of the number of particles N, but the HS for all of them.

With this, we have shown numerically that the previous protocol can be improved, to the point that one can reach HS. That is, still there are better ways to perform magnetometry, even in the symmetric space and in this particular setting. Moreover, this is still done with fairly simple control Hamiltonians and without time control interactions.

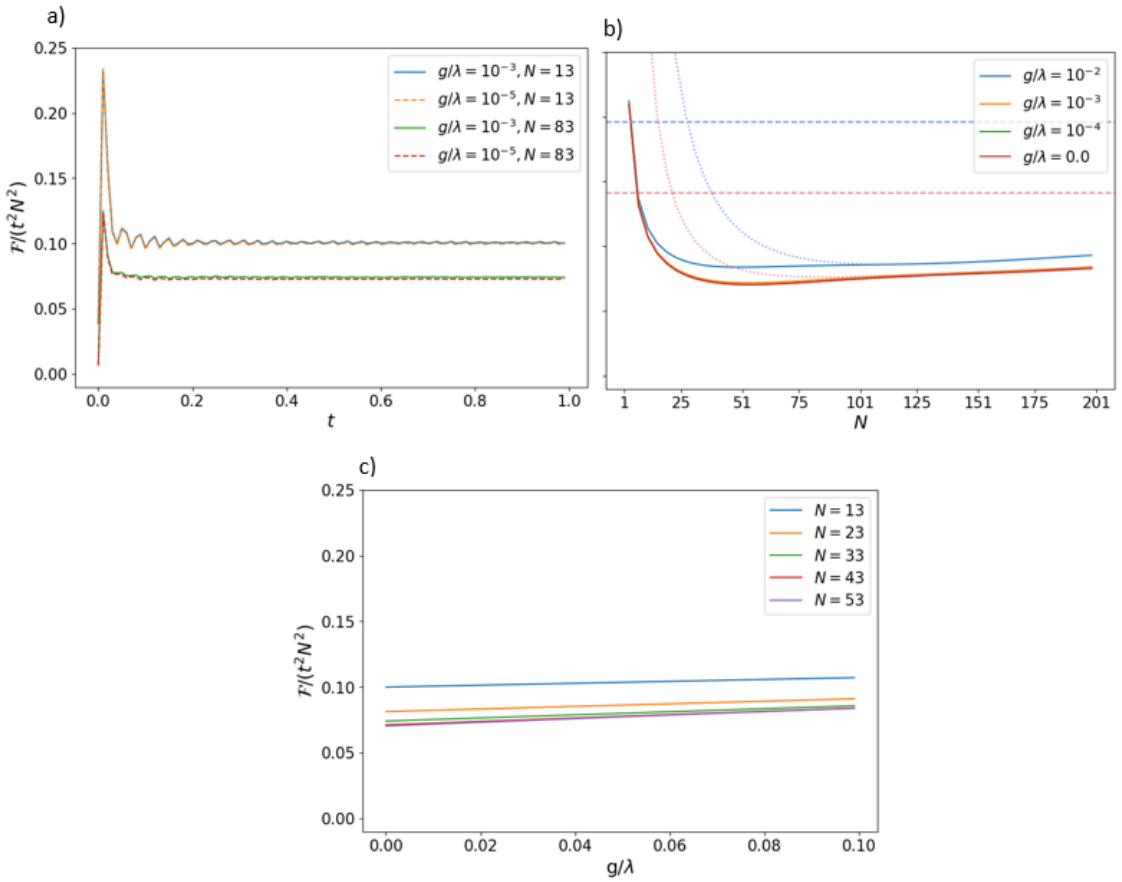

Figure 7: Representation of the different relations of $\mathcal{F}/(t^2N^2)$ with respect to important parameters of the problem. Figures (b,c) are studied in the long time regime. With the re-scaling it seems that HS is achieved. (a) Relation of $\mathcal{F}/(t^2N^2)$ with t (in natural units) for two radically different values of $\frac{g}{\lambda}$ and N. It can be seen that both parameters have a negligent effect on reaching the "steady state". (b) Relation between the $\mathcal{F}/(t^2N^2)$ and the number of particles used (recall that N is always odd) for different relations between g/λ. Here is where the apparent HS is most obvious. Two regression functions (shown in dotted lines) of the form $f(N) = a + b/\sqrt{N} + c/N$ are shown with their asymptotic convergence (in dashed lines). This are for $g = 0$ in red, and $g = 10^{-2}$ in blue. The regressions are $f_{g=0}(N) = 0.141 - 1.193/\sqrt{N} + 5.498/N$, $f_{g=10^{-2}}(N) = 0.196 - 2.311/\sqrt{N} + 12.159/N$ (c) Relation between $\mathcal{F}/(t^2N^2)$ and g/λ for the different number of particles N. This figure highlights the fact that the QFI is almost with respect to the relation between g/λ.

7 Conclusions

In this thesis, we have studied a different setting to perform quantum metrology with a special focus in magnetometry.

The usual setting to extract information of a parameter in a magnetic field consists of the following steps: prepare a sensor into a carefully engineered quantum state, let the state interact with the magnetic field and finally measure the state (as shown in Fig. 3a). In this project we have focused on exploiting interacting many-body dynamics to entangle a state while a magnetic field encodes its information into it (Fig. 3b). With this approach, we avoid the preparation of the state, and thus, circumvent the different problems that come with this. With this approach, we have shown that the SNL can be surpassed and therefore have a quantum advantage in the amount of information gained for each measurement. Or in other words, we show that a QFI higher than the $\mathcal{F}_{SNL} = t^2 N$ is achieved.

This new approach opens new doors to tackle new challenges in the field of quantum metrology. Particularly, on those that arise when trying to achieve a quantum advantage in the QFI. Indeed this approach might help reduce the overall time of the protocols that require a previous state preparation, reduce the time control required to prepare highly entangled states, as well as potentially being more resistant to noise and decoherence. The results obtained in this thesis are summarized below.

Firstly, in Section 4 we prove a new expression for the QFI for pure states. In the long time regime we get the same well known $\mathcal{F} = 4t^2(\Delta H_p)_{\rho_0}$, where the generator S_z is replaced by its pinched version $H_p = \sum_k P_k S_z P_k$. Also, it helps into understanding how to achieve HS. By means of entangling the eigenstates of the Hamiltonian via the projectors of the Hamiltonian, instead of having an entangled initial state. Firstly, this expression is very similar to the QFI for the standard protocol and pure states. Secondly, it is time independent (under the assumption of large times).

Secondly, in Section 5 we present a novel protocol to achieve a quantum advantage proportional to HS. Using many-body interactions we can achieve a fraction of the maximum value of the QFI. Thus achieving the maximum scaling of $\mathcal{F} \sim t^2 N^2$. This is very important, as it shows the feasibility of this new approach (Fig. 3b).

Motivated by the possibility of implementing this approach experimentally, in Section 6 we study two body interactions to create entanglement. In this case, we showed that a one-axis twisting term is enough to create a quantum advantage when the interacting strength is much larger than the value of the estimated parameter. It also requires an odd number of particles. This quantum advantage is of order $\mathcal{F} \sim t^2 N^{3/2}$.The approximation has been studied numerically to see that it holds for different values of $t,\ N,\ g/\lambda$, the three important parameters of this study. Finally, it has been shown that a feasible measurement of S_x is enough to achieve this value of the QFI. Moreover, this result has been compared to other results in the literature for a similar protocol using the two step process of preparing and interacting the state (in Fig. 3a) with the signal. This highlighted the main differences between the two protocols.

In Section 6 we have also done a gradient-based optimization of the QFI using *Pytorch* [PGM+19]. This consists of a gradien-based optimization of four parameters of $\theta, \phi, \alpha, \beta$. With this we have shown numerically that for a certain value, a better QFI than the previous two body protocol can be achieved. This has also been studied numerically to show that it holds even better than the previous two body protocol. Indeed, we have found that even the scaling changes, achieving HS $\mathcal{F} \sim N^2 t^2$.

In conclusion, studying this framework has resulted in a new expression for the QFI, as well as showing that a quantum advantage is attainable in different settings. Even though

full HS has not been achieved ($\mathcal{F} = N^2t^2$), particular approaches that might be more feasible to implement have been shown and studied. This thesis opens new doors for the further study and development of quantum-enhanced estimation protocols, by developing an alternative approach that is able to eliminate time control required in the established protocol and reduce its overall time. Potentially, it might be more robust to noise and decoherence.

8 Ongoing work & outlook

A crucial issue that has not been tackled in this work is robustness to noise. Indeed, for the standard approach (Fig. 3a) there have been some recent results showing that decoherence prevents Heisenberg scaling, in fact bounding it to shot-noise scaling [DDKG12]. Interestingly, these results do not necessarily apply to our approach (Fig. 3b) due to the presence of interactions. An important open question is to characterise the robustness of the quantum advantages under decoherence and noise. Moreover, it has been shown that entangled states can be created even under the presence of dissipative evolution [ZV21]. Therefore, the presence of interactions suggests an exciting open direction: can dissipative dynamics be exploited to create useful states for sensing?

A challenging future endeavour is to characterize the potential for metrology of standard many-body systems, which feature two-body local interactions. An example of such interaction is a spin chain in which every particle only interacts with its closest neighbours. Luckily there are already some tools developed to ease this process. These are Matrix Product Operators (MPO) and Matrix Product States (MPS), fundamental tools from Tensor Networks. Because of the already discussed flatness of the QFI, using greedy searches might not be enough. Thus the strategy would be to assume some form of the Hamiltonians that generate the interactions using MPO and then optimize those with the implementation of optimization methods such as the one used in this thesis.

Bibliography

[A+16] B. P. Abbott et al. Observation of gravitational waves from a binary black hole merger. *Physical Review Letters*, 116(6), Feb 2016.

[AKS+16] R. Augusiak, J. Kołodyń ski, A. Streltsov, M. N. Bera, A. Acín, and M. Lewenstein. Asymptotic role of entanglement in quantum metrology. *Physical Review A*, 94(1), Jul 2016.

[BC94a] S. L. Braunstein and C. M. Caves. Statistical distance and the geometry of quantum states. *Phys. Rev. Lett.*, 72:3439–3443, May 1994.

[BC94b] S. L. Braunstein and C. M. Caves. Statistical distance and the geometry of quantum states. *Phys. Rev. Lett.*, 72:3439–3443, May 1994.

[Cra46] H. Cramér. *Mathematical methods of statistics / by Harald Cramér*. Princeton mathematical series ; 9. Princeton University Press, Princeton, 1946.

[DDJK15] R. Demkowicz-Dobrzański, M. Jarzyna, and J. Kołodyński. Quantum limits in optical interferometry. In *Progress in Optics*, pages 345–435. Elsevier, 2015.

[DDKG12] R. Demkowicz-Dobrzański, J. Kołodyński, and M. GuŢă. The elusive heisenberg limit in quantum-enhanced metrology. *Nature Communications*, 3(1):1063, Sep 2012.

[GHSZ90] D. M. Greenberger, M. A. Horne, A. Shimony, and A. Zeilinger. Bell's theorem without inequalities. *American Journal of Physics*, 58(12):1131–1143, Dec 1990.

[GLM06] V. Giovannetti, S. Lloyd, and L. Maccone. Quantum metrology. *Physical Review Letters*, 96(1), Jan 2006.

[GLM11] V. Giovannetti, S. Lloyd, and L. Maccone. Advances in quantum metrology. *Nature Photonics*, 5(4):222–229, Mar 2011.

[HHR+05] H. Häffner, W. Hänsel, C. F. Roos, J. Benhelm, D. Chek al kar, M. Chwalla, T. Körber, U. D. Rapol, M. Riebe, P. O. Schmidt, C. Becher, O. Gühne, W. Dür, and R. Blatt. Scalable multiparticle entanglement of trapped ions. *Nature*, 438(7068):643–646, Dec 2005.

[KB17] D. P. Kingma and J. Ba. Adam: A method for stochastic optimization, 2017.

[KKAR03] I. K. Kominis, T. W. Kornack, J. C. Allred, and M. V. Romalis. A subfemtotesla multichannel atomic magnetometer. *Nature*, 422(6932):596–599, Apr 2003.

[LBY+15] A. D. Ludlow, M. M. Boyd, J. Ye, E. Peik, and P. O. Schmidt. Optical atomic clocks, 2015.

[MCBS22] R. Muñoz, J. Calsamiglia, E. Bagan, and G. Santís. Quantum statistical inference lecture notes, 2022.

[MLS04] M. W. Mitchell, J. S. Lundeen, and A. M. Steinberg. Super-resolving phase measurements with a multiphoton entangled state. *Nature*, 429(6988):161–164, May 2004.

[MWSN11] J. Ma, X. Wang, C.P. Sun, and F. Nori. Quantum spin squeezing. *Physics Reports*, 509(2-3):89–165, Dec 2011.

[NC10] M.A. Nielsen and I. L. Chuang. *Quantum Computation and Quantum Information: 10th Anniversary Edition*. Cambridge University Press, 2010.

[PGM+19] A. Paszke, S. Gross, F. Massa, A. Lerer, J. Bradbury, G. Chanan, T. Killeen, Z. Lin, N. Gimelshein, L. Antiga, A. Desmaison, A. Köpf, A. Yang, Z. DeVito, M. Raison, A. Tejani, S. Chilamkurthy, B. Steiner, L. Fang, J. Bai, and S. Chintala. Pytorch: An imperative style, high-performance deep learning library, 2019.

[Pre14] J. Preskill. Lecture notes for physics 219: Quantum computaion, Jun 2014.

[PS09] L. Pezzé and A. Smerzi. Entanglement, nonlinear dynamics, and the heisenberg limit. *Physical Review Letters*, 102(10), Mar 2009.

[PSO+18] L Pezzè, A. Smerzi, M. K. Oberthaler, R. Schmied, and P. Treutlein. Quantum metrology with nonclassical states of atomic ensembles. *Reviews of Modern Physics*, 90(3), Sep 2018.

[SN13] J. J Sakurai and J. Napolitano. *Modern Quantum Mechanics*. Pearson Education UK, Harlow, 2013.

[TA14] G. Tóth and I. Apellaniz. Quantum metrology from a quantum information science perspective. *Journal of Physics A: Mathematical and Theoretical*, 47(42):424006, Oct 2014.

[Wil67] R. M. Wilcox. Exponential Operators and Parameter Differentiation in Quantum Physics. *J. Math. Phys.*, 8:962–982, 1967.

[WJK+10] W. Wasilewski, K. Jensen, H. Krauter, J. J. Renema, M. V. Balabas, and E. S. Polzik. Quantum noise limited and entanglement-assisted magnetometry. *Physical Review Letters*, 104(13), Mar 2010.

[ZV21] S. Zippilli and D. Vitali. Dissipative engineering of gaussian entangled states in harmonic lattices with a single-site squeezed reservoir. *Physical Review Letters*, 126(2), Jan 2021.

A Proof: Quantum Fisher Information for the long time regime

Let us start by defining the setting. Let us have an state $|\rho_g\rangle = e^{-itH(g)}|\rho_0\rangle$, where $H = gS_z + \sum_j \lambda_j + h_j$ ($\{\lambda_j\}$ are control parameters and $\{h_j\}$ are the associated operators). Now to compute the QFI $\mathcal{F}$, Eq. (15) is used:

$$\mathcal{F} = 4(\langle\dot{\rho}_g|\dot{\rho}_g\rangle - |\langle\dot{\rho}_g|\rho_g\rangle|) \tag{33}$$

Also to compute $|\dot{\rho}_g\rangle$, Eq. (20) is used. Let E_k be the energies of H, P_k be the projector of H (notice how the projectors include all the degeneracy, that is $P_k = \sum_i \left|E_k^{(i)}\right\rangle\!\left\langle E_k^{(i)}\right|$, where (i) accounts for the degenerate orthogonal states in the subspace), then if we write $e^{-itH(g)} = \sum_k P_k e^{-itE_k}$

$$\begin{aligned}
|\dot{\rho}_g\rangle =& -it\int_0^1 \sum_k^N e^{-istE_k} P_k S_z \sum_j^N e^{-it(1-s)E_j} P_j ds\,|\rho_0\rangle = \\
=& -it\sum_{k,j}^N P_k S_z P_j \int_0^1 e^{-it(E_j-(E_j-E_k)s)} ds\,|\rho_0\rangle = \\
=& -it\sum_k^N P_k S_z P_k e^{-itE_k}|\rho_0\rangle + \sum_{k,j|j\neq k}^N \frac{e^{-itE_k}-e^{-itE_j}}{E_k-E_j} P_k S_z P_k|\rho_0\rangle \approx \\
\overset{(A)}{\approx}& -it\sum_k^N P_k S_z P_k e^{-itE_k}|\rho_0\rangle = -itH_p|\rho_g\rangle \ ,
\end{aligned} \tag{34}$$

where in (A) the largest order in t is kept. This is motivated because the leading term in the QFI will go with the time squared. Moreover, the terms that are not considered are bounded with the inverse of $\Delta E = \min_E |E_k - E_l|$. Also, in the last inequality, it has been defined $H_p := \sum_k P_k S_z P_k$.

From this point on-wards is just a matter of substituting this result into Eq. (15). The first term will look like

$$\begin{aligned}
\langle\dot{\rho}_g|\dot{\rho}_g\rangle =& t^2\langle\rho_g|H_p^2|\rho_g\rangle = t^2\langle\rho_0|U^\dagger H_p^2 U|\rho_0\rangle = \\
=& t^2\langle\rho_0|\sum_l^N P_l S_z P_l e^{+itE_l}\sum_k^N P_k S_z P_k e^{-itE_k}|\rho_0\rangle = \\
=& t^2\langle\rho_0|\sum_k^N P_k S_z P_k S_z P_k|\rho_0\rangle = t^2\langle\rho_0|H_p^2|\rho_0\rangle \ .
\end{aligned} \tag{35}$$

And the second

$$\begin{aligned}
\langle\dot{\rho}_g|\rho_g\rangle =& it\langle\rho_g|H_p|\rho_g\rangle = \langle\rho_0|U^\dagger H_p U|\rho_0\rangle = \\
=& it\langle\rho_0|\sum_l^N P_l e^{itE_l}\sum_k^N P_k S_z P_k e^{-itE_k}|\rho_0\rangle = \\
=& it\langle\rho_0|H_p|\rho_0\rangle \ ,
\end{aligned} \tag{36}$$

thus

$$\mathcal{F} = 4t^2(\Delta H_p)^2_{|\rho_0\rangle} + \mathcal{O}(t) \ . \tag{37}$$

□

B Proof: Achieving Heisenberg Scaling with many-body interactions

For this proof we require to choose a setting that allows us to achieve Heisenberg Scaling. Let us have an state $|\rho_g\rangle = e^{-itH(g)}|\rho_0\rangle$, where $H = gS_z + \sum_j \lambda_j + h_j$ ($\{\lambda_j\}$ are control parameters and $\{h_j\}$ are the associated operators). Let us choose (with an even number of spins) the following setting

$$\sum_j \lambda_j h_j = N\lambda\left(|N\rangle\langle 0| + |0\rangle\langle N| + |-N\rangle\langle 0| + |0\rangle\langle -N|\right) \ , \tag{38}$$

where $S_z|N\rangle = N,\ S_z|-N\rangle = -N|-N\rangle,\ S_z|0\rangle = 0$ (i.e. the state with all spins pointing up, down and with the same number up and down). Now assume that we choose a state that lives in the subspace generated by $|N\rangle, |-N\rangle, |0\rangle$. Then H_p can be reduced to this subspace without loss of generality in the QFI.

Therefore, we can define an effective Hamiltonian $H' = \frac{N}{2}|N\rangle\langle N| + \frac{-N}{2}|-N\rangle\langle -N| + N\lambda\left(|N\rangle\langle 0| + |0\rangle\langle N| + |-N\rangle\langle 0| + |0\rangle\langle -N|\right)$. The eigenstates of this H' are

$$\begin{aligned}
|E_1\rangle =& \frac{-\lambda}{\sqrt{g^2+2\lambda^2}}|N\rangle + \frac{g}{\sqrt{g^2+2\lambda^2}}|0\rangle + \frac{\lambda}{\sqrt{g^2+2\lambda^2}}|-N\rangle \ , \\
|E_2\rangle =& \frac{1}{\sqrt{a_+^2+\lambda^2 b_+^2+\lambda^4}}\left(a_+|N\rangle + \lambda b_+|0\rangle + \lambda^2|-N\rangle\right) \ , \\
|E_3\rangle =& \frac{1}{\sqrt{a_-^2+\lambda^2 b_-^2+\lambda^4}}\left(a_-|N\rangle + \lambda b_-|0\rangle + \lambda^2|-N\rangle\right) \ ,
\end{aligned} \tag{39}$$

with $a_\pm = g^2+\lambda^2 \pm g\sqrt{g^2+2\lambda^2},\ b_\pm = g \pm \sqrt{g^2+2\lambda^2}$. Because this space is now not degenerate, one can compute the expected values of the three eigenvectors with respect to S_z and obtain

$$\begin{aligned}
\langle E_1|S_z|E_1\rangle =& 0 \ , \\
\langle E_2|S_z|E_2\rangle =& \frac{N}{2}\frac{a_+^2-4\lambda^2}{a_+^2+\lambda^2 b_+^2+\lambda^4} \ , \\
\langle E_3|S_z|E_3\rangle =& \frac{N}{2}\frac{a_-^2-4\lambda^2}{a_-^2+\lambda^2 b_-^2+\lambda^4} \ .
\end{aligned} \tag{40}$$

Finally, by choosing as your initial state $|0\rangle$, one finds that

$$\mathcal{F} = 4t^2N^2\frac{g^2\lambda^2}{(g^2+2\lambda^2)^2} \ , \tag{41}$$

with a maximum in $\lambda = \frac{g}{\sqrt{2}}$, that achieves $\mathcal{F} = \frac{1}{2}t^2N^2$. □

Notice how if $g \to 0$ it might seem that the protocol will fail, however, one can always define a $g' = g + c$ where c is a constant that can be introduced by adding a term cJ_z in H.

C Proof: Quantum Advantage with two body interactions

Let us have an state $|\rho_g\rangle = e^{-itH(g)}|\rho_0\rangle$, where $H = gS_z + \sum_s \lambda_j + h_j$ ($\{\lambda_j\}$ are control parameters and $\{h_j\}$ are the associated operators). Let $H = \lambda S_x^2 + gS_z$, then let $\{|s_x, m\rangle\}$ be the eigenvectors of S_x (thus also S_x^2), where m represents the eigenvalue of S_x. Then at first order

$$|s_x, m\rangle^{(1)} = |s_x, m\rangle + \frac{g}{\lambda}\sum_{k,s}\frac{\langle s_x, l|\, S_z\, |s_x, m\rangle}{m^2 - l^2}|s_x, l\rangle \ . \tag{42}$$

Then, for any number of particles $N = 2s_x$, except for the subspace of $m^2 = 1/4$ (when we have an odd number of particles N), we can never find a basis that behaves like

$$\langle s_x, m|\, S_z\, |s_x, \pm m\rangle \propto \delta_{m,\pm m} \ , \tag{43}$$

in any degenerate subspace. Thus any

$$P_k S_z P_k = \mathcal{O}\left(\frac{g}{\lambda}\right) , \tag{44}$$

that is because if we take the first correction of the eigenvectors $|s_x, m\rangle^{(1)}$

$$\begin{aligned} \langle s_x, m|^{(1)}\, S_z\, |s_x, \pm m\rangle^{(1)} &= \cancelto{0,\ (a)}{\langle s_x, m|\, S_z\, |s_x, \pm m\rangle} + \\ + \frac{g}{\lambda}\sum_{l,l'|l'=\pm m}\frac{\langle s_x, l|\, S_z\, |s_x, l'\rangle}{m^2 - l^2}\langle s_x, \mp l'|\, S_z\, |s_x, l\rangle + \mathcal{O}\left(\frac{g^2}{\lambda^2}\right) , \end{aligned} \tag{45}$$

where in (a) we are using Eq. (43).

Now let us see what happens for the case of $m^2 = \frac{1}{4}$. First notice that the state that behaves like Eq. (43) is $|s_x, \pm\rangle = \frac{1}{\sqrt{2}}\left(\left|s_x, m = \frac{1}{2}\right\rangle \pm \left|s_x, m = \frac{-1}{2}\right\rangle\right)$. Now let us see that this state breaks the degeneracy in energy in this space

$$E_\pm^{(1)} = E + \langle s_x, \pm|S_z|s_x, \pm\rangle = E \pm \frac{g}{2\lambda}\sqrt{s(s+1) - \frac{1}{4}} \ , \tag{46}$$

thus

$$\begin{aligned} H_P = \sum_{k=\pm} P_k S_z P_k =& \frac{1}{2}\sqrt{s(s+1) - \frac{1}{4}}\left(|s_x, +\rangle\langle s_x, +| - |s_x, -\rangle\langle s_x, -|\right) + \mathcal{O}(\tfrac{g}{\lambda}) = \\ =& \frac{1}{2}\sqrt{s(s+1) - \frac{1}{4}}\left(\left|s_x, \frac{+1}{2}\right\rangle\left\langle s_x, \frac{-1}{2}\right| + \left|s_x, \frac{-1}{2}\right\rangle\left\langle s_x, \frac{+1}{2}\right|\right) + \mathcal{O}\left(\frac{g}{\lambda}\right) . \end{aligned} \tag{47}$$

Then using the following state as our initial state[26], one sees that for $\eta = -\tan\left(\frac{\theta}{2}\right)e^{-i\phi}$

$$|\eta\rangle = |\theta_x, \phi_x\rangle^{\otimes N} = \frac{1}{(1+|\eta|^2)^s}\sum_{m=-s}^{s}\binom{2s}{s+m}^{1/2}\eta^{s+m}|s_x, m\rangle \ . \tag{48}$$

And to compute $\mathcal{F} = 4t^2(\Delta H_P)_\eta^2$ at 0-th order in $\frac{g}{\lambda}$, let us first

$$\begin{aligned} \langle\eta|H_P^2|\eta\rangle = \frac{1}{4}\left(s(s+1) - \frac{1}{4}\right)\langle\eta|\left(\left|\frac{+1}{2}\right\rangle\left\langle\frac{+1}{2}\right| + \left|\frac{-1}{2}\right\rangle\left\langle\frac{-1}{2}\right|\right)|\eta\rangle = \\ = \frac{1}{4}\left(s(s+1) - \frac{1}{4}\right)\frac{|\eta|^{2k}}{(1+|\eta|^2)^{2k}}\binom{2k+1}{k} , \end{aligned} \tag{49}$$

[26] This is a product state made of N Block Vectors pointing in the same direction[MWSN11].

where $s = \frac{2k+1}{2}$ because

$$\left|\left\langle \eta \middle| \frac{1}{2} \right\rangle\right|^2 = \frac{1}{(1+|\eta|^2)^{2s}} |\eta|^{2s+1} \binom{2s}{s+\frac{1}{2}} =$$
$$\overset{(A)}{=} \frac{|\eta|^{2k+2}}{(1+|\eta|^2)^{2k+1}} \binom{2k+1}{k+1} = \tag{50}$$
$$= \frac{|\eta|^{2k+2}}{(1+|\eta|^2)^{2k+1}} \binom{2k+1}{k} \cancelto{1}{\left(\frac{2k+1-k-1+1}{k+1}\right)},$$

where in (A) it has been used that $s = \frac{2k+1}{2}$. Also

$$\left|\left\langle \eta \middle| \frac{-1}{2} \right\rangle\right|^2 = \frac{|\eta|^{2k}}{(1+|\eta|^2)^{2k+1}} \binom{2k+1}{k} . \tag{51}$$

Now we also need

$$\langle \eta | H_P | \eta \rangle = -\sqrt{s(s+1) - \frac{1}{4}} \frac{|\eta|^{2k}}{(1+|\eta|^2)^{2k+1}} \tan\frac{\theta_x}{2} \cos\phi_x \ . \tag{52}$$

That is because

$$\left\langle \eta \middle| \frac{1}{2} \right\rangle \left\langle \frac{-1}{2} \middle| \eta \right\rangle = \frac{|\eta|^{2k}\eta^*}{(1+|\eta|^2)^{2k+1}} \binom{2k+1}{k} . \tag{53}$$

Then if $\phi_x = \frac{\pi}{2}$, $(\Delta H_P) = \frac{1}{4}\left(s(s+1) - \frac{1}{4}\right) \frac{|\eta|^{2k}}{(1+|\eta|^2)^{2k}} \binom{2k+1}{k}$, that is

$$\mathcal{F} = t^2 \left((2k+1)(2k+3) - \frac{1}{4}\right) \frac{1}{2^{2k}} \binom{2k+1}{k} + \mathcal{O}\left(\frac{g}{\lambda}\right) \ , \tag{54}$$

now, for $|\eta|^2 = 1$ this expression is maximal, thus

$$\max_{\theta,\phi} \mathcal{F} = t^2 \left(k(k+2) + \frac{1}{2}\right) \frac{1}{2^{2k}} \binom{2k+1}{k} + \mathcal{O}\left(\frac{g}{\lambda}\right) \ , \tag{55}$$

and this for large k, i.e. large but odd s,

$$\mathcal{F} = t^2 \frac{2k^{3/2}}{\sqrt{\pi}} + \mathcal{O}\left(\frac{g}{\lambda}\right) \Rightarrow \mathcal{F} = t^2 \frac{N^{3/2}}{\sqrt{2\pi}} + \mathcal{O}\left(\frac{g}{\lambda}\right) \ . \tag{56}$$

□

D Proof: Quantum Advantage with local observables

Let us have an state $|\rho_g\rangle = e^{-itH(g)}|\rho_0\rangle$, where $H = gS_z + \sum_j \lambda_j + h_j$ ($\{\lambda_j\}$ are control parameters and $\{h_j\}$ are the associated operators). Let $H = \lambda J_x^2 + gJ_z$. Let the measurement performed be $M = J_x$. Recall now the definition of the eigenstates of H_p (the Pinched Hamiltonian)[27]

$$|j_x, \pm\rangle = \frac{1}{\sqrt{2}}\left(\left|j_x, m = \frac{1}{2}\right\rangle \pm \left|j_x, m = \frac{-1}{2}\right\rangle\right) . \tag{57}$$

Also, it is important to point out that the states

$$\left|j_x, m = \frac{1}{2}\right\rangle, \left|j_x, m = \frac{-1}{2}\right\rangle , \tag{58}$$

are non-degenerate states of J_x.

Finally, this two states are the ones that span the space of H_p. Therefore, recalling Eq. (10), this subspace will be enough to compute the classical FI. That is, if

$$\left|j_x, \pm\frac{1}{2}\right\rangle = \frac{1}{\sqrt{2}}\left(|j_x, +\rangle \pm i\,|j_x, -\rangle\right) . \tag{59}$$

Then the FI will be

$$F = \frac{t^2\,\mathrm{Tr}\left\{i\left[\left|j_x, \frac{1}{2}\right\rangle\!\left\langle j_x, \frac{1}{2}\right|, H_p\right]\rho\right\}^2}{\mathrm{Tr}\left\{\left|j_x, \frac{1}{2}\right\rangle\!\left\langle j_x, \frac{1}{2}\right|\rho\right\}} + \frac{t^2\,\mathrm{Tr}\left\{i\left[\left|j_x, \frac{-1}{2}\right\rangle\!\left\langle j_x, \frac{-1}{2}\right|, H_p\right]\rho\right\}^2}{\mathrm{Tr}\left\{\left|j_x, \frac{-1}{2}\right\rangle\!\left\langle j_x, \frac{-1}{2}\right|\rho\right\}} + \mathcal{O}\left(\frac{g}{\lambda}\right) , \tag{60}$$

where $\rho = |\rho_g\rangle\langle\rho_g|$ and $[A, B] = AB - BA$. Now its easy to see that

$$\begin{aligned} \left|j_x, \frac{1}{2}\right\rangle\!\left\langle j_x, \frac{1}{2}\right| \left(|j_x, +\rangle\langle j_x, +| - |j_x, -\rangle\langle j_x, -|\right) &= \left|j_x, \frac{1}{2}\right\rangle\!\left\langle j_x, \frac{-1}{2}\right| , \\ \left(|j_x, +\rangle\langle j_x, +| - |j_x, -\rangle\langle j_x, -|\right) \left|j_x, \frac{1}{2}\right\rangle\!\left\langle j_x, \frac{1}{2}\right| &= \left|j_x, \frac{-1}{2}\right\rangle\!\left\langle j_x, \frac{+1}{2}\right| . \end{aligned} \tag{61}$$

Thus subtracting this terms, one can rewrite it as

$$\left|j_x, \frac{1}{2}\right\rangle\!\left\langle j_x, \frac{-1}{2}\right| - \left|j_x, \frac{-1}{2}\right\rangle\!\left\langle j_x, \frac{+1}{2}\right| = \left(|j_x, -\rangle\langle j_x, +| - |j_x, +\rangle\langle j_x, -|\right) . \tag{62}$$

Similarly, the same result is obtained from $|y, -\rangle\langle y, -|$, up to a sign. Therefore if $c = \sqrt{j_x(j_x+1) - \frac{1}{4}}$

$$\begin{aligned} F =& \frac{t^2c^2\,\mathrm{Tr}\{i\left(|j_x, +\rangle\langle j_x, -| - |j_x, -\rangle\langle j_x, +|\right)\rho\}^2}{\mathrm{Tr}\left\{\left|j_x, \frac{1}{2}\right\rangle\!\left\langle j_x, \frac{1}{2}\right|\rho\right\}} \\ &+ \frac{t^2c^2\,\mathrm{Tr}\{i\left(|j_x, +\rangle\langle j_x, -| - |j_x, -\rangle\langle j_x, +|\right)\rho\}^2}{\mathrm{Tr}\left\{\left|j_x, \frac{-1}{2}\right\rangle\!\left\langle j_x, \frac{-1}{2}\right|\rho\right\}} + \mathcal{O}\left(\frac{g}{\lambda}\right) . \end{aligned} \tag{63}$$

Recalling that the state being used is $|y\rangle^{\otimes N}$, i.e. a product of Bloch Sphere states pointing in the y direction, and using that this can be written as in Eq. (48) this proof can continue.

[27] See Annex C for the proof.

$$\mathrm{Tr}\{i\left(|j_x,+\rangle\langle j_x,-|-|j_x,-\rangle\langle j_x,+|\right)\rho\} = ie^{it\frac{g}{\lambda}c}\langle j_x,+|\,\rho_0\,|j_x,-\rangle - ie^{-it\frac{g}{\lambda}c}\langle j_x,-|\,\rho_0\,|j_x,+\rangle \ . \tag{64}$$

And using the notation of the previous proof

$$\begin{aligned}\langle j_x,+|\rho_0\rangle &= \frac{1}{\sqrt{2}2^j} i^k (i+1)\sqrt{\binom{2k+1}{k}}\ ,\\ \langle j_x,+|\rho_0\rangle &= \frac{1}{\sqrt{2}2^j} i^k (i-1)\sqrt{\binom{2k+1}{k}}\ .\end{aligned} \tag{65}$$

Therefore

$$\begin{aligned}\langle j_x,+|\,\rho_0\,|j_x,-\rangle &= \frac{-i}{2^{2j}}\binom{2k+1}{k}\ ,\\ \langle j_x,-|\,\rho_0\,|j_x,+\rangle &= \frac{+i}{2^{2j}}\binom{2k+1}{k}\ .\end{aligned} \tag{66}$$

To finally obtain

$$\mathrm{Tr}\{i\left(|j_x,+\rangle\langle j_x,-|-|j_x,-\rangle\langle j_x,+|\right)\rho\} = \frac{1}{2^{2j}}\binom{2k+1}{k} 2\cos\left(t\frac{g}{\lambda}c\right)\ . \tag{67}$$

Now, there is only part left is to compute

$$\mathrm{Tr}\left\{\left|j_x,\pm\frac{1}{2}\right\rangle\!\left\langle j_x,\pm\frac{1}{2}\right|\rho\right\}\ . \tag{68}$$

By rewriting

$$\left|j_x,\pm\frac{1}{2}\right\rangle\!\left\langle j_x,\pm\frac{1}{2}\right| = |j_x,+\rangle\langle j_x,+| + |j_x,-\rangle\langle j_x,-| \pm \left(|j_x,+\rangle\langle j_x,-| + |j_x,-\rangle\langle j_x,+|\right)\ , \tag{69}$$

it is easy to see that

$$\mathrm{Tr}\{\left(|j_x,+\rangle\langle j_x,+| + |j_x,-\rangle\langle j_x,-|\right)\rho\} = \frac{2}{2^{2j}}\binom{2k+1}{k}\ , \tag{70}$$

and

$$\pm\,\mathrm{Tr}\{\left(|j_x,-\rangle\langle j_x,+| - |j_x,+\rangle\langle j_x,-|\right)\rho\} = \pm\frac{1}{2^{2j}}\binom{2k+1}{k} 2\sin\left(t\frac{g}{\lambda}c\right)\ . \tag{71}$$

Substituting everything in the FI

$$\begin{aligned}F =& \frac{2t^2c^2}{2^{2j}}\binom{2k+1}{k}\cos^2\left(t\frac{g}{\lambda}c\right)\left(\frac{1}{1-\sin\left(t\frac{g}{\lambda}c\right)}+\frac{1}{1+\sin\left(t\frac{g}{\lambda}c\right)}\right)+\mathcal{O}\left(\frac{g}{\lambda}\right)=\\ =& t^2c^2\frac{1}{2^{2k}}\binom{2k+1}{k}+\mathcal{O}\left(\frac{g}{\lambda}\right)=\mathcal{F}\ .\end{aligned} \tag{72}$$

□

E Code: Optimization of the Quantum Fisher Information using generalized angular momentum matrices.

```
########################## Import the necessary packages
#### Math
import numpy as np
from scipy import linalg
from scipy import special
from IPython.display import clear_output
from scipy.linalg import expm, sinm, cosm

#### Plots
import matplotlib.pyplot as plt

#### Machine Learning
import torch
import torch.nn as nn
import torch.optim as optim

########################## Define the vector
def state(theta,phi,N):
    A = N*torch.ones(N+1)-(torch.arange(N+1))
    eta=-torch.tan(theta/2)*torch.exp(-1j*phi)
    return eta**A/(1+eta*eta.conj())**(N/2)*vec_binom

########################## Define the matrices
def H(N):
    Jz=torch.zeros((N+1,N+1),dtype = torch.complex128)
    Jp=torch.zeros((N+1,N+1),dtype = torch.complex128)
    Jm=torch.zeros((N+1,N+1),dtype = torch.complex128)
    for i in range(int(N/2)+1):
        Jz[i,i]=(N-2*i)/2
        Jz[N-i,N-i]=-(N-2*i)/2


        Jp[i,i+1]=np.sqrt(N/2*(N/2+1)-(N-2*i)/2*((N-2*i)/2-1))
        Jp[N-i-1,N-i]=np.sqrt(N/2*(N/2+1)-(N-2*i)/2*((N-2*i)/2-1))

        Jm[i+1,i]=np.sqrt(N/2*(N/2+1)-(N-2*i)/2*((N-2*i)/2-1))
        Jm[N-i,N-i-1]=np.sqrt(N/2*(N/2+1)-(N-2*i)/2*((N-2*i)/2-1))

    Jx=0.5*(Jp+Jm)
    Jy=-1j*0.5*(Jp-Jm)

    return Jx,Jy,Jz

########################## Define the Loss Function (class object)
class LossFunction(nn.Module):
    def __init__(self, Jxx,Jyy,Jz,dim, t,g,N):
```

```
47          super().__init__()
48
49          #parameter to be estimated
50          self.g = g
51
52          #parameters that will be used to compute the derivative of the
            ↪  fisher
53          self.g1 = torch.tensor(g, requires_grad=True)
54          self.g2 = torch.tensor(g, requires_grad=True)
55
56          #actual parameters to optimize over
57          self.theta_vec = nn.Parameter(torch.rand(4), requires_grad=True)
58
59          #various definitions for the class
60          self.Jxx = Jxx
61          self.Jyy = Jyy
62          self.Jz = Jz
63          self.N = N
64          self.dim = dim
65          self.t = t
66
67      #Forward is a function that must be implemented, and determines what
        ↪  is returned when this object is called (value of the loss
        ↪  function).
68      def forward(self):
69
70          vec=state(self.theta_vec[0],self.theta_vec[1],self.N)
71          H1=self.Jz * self.g1
72          H2=self.Jz * self.g2
73          H=self.Jz * self.g
74          Hh =
            ↪  self.Jxx*self.theta_vec[2]+self.Jyy*self.theta_vec[3]/np.sqrt(self.N)
75
76          #define the Hamiltonian
77          H = H + Hh
78          H1 = H1 + Hh
79          H2 = H2 + Hh
80
81          #define the unitary evolution
82          U = torch.matrix_exp(-1j*t*H)@vec
83          U1 = torch.matrix_exp(-1j*t*H1)@vec
84          U2 = torch.matrix_exp(-1j*t*H2)@vec
85
86          #- quantum fisher
87          loss = - 4*100 *
            ↪  torch.real(U1.conj()@U2-(U.conj()@U1)*(U2.conj()@U))/(t*t*N**(2))
88
89          #make the derivatives using pythorch, more precise
```

```
        dg1_loss = torch.autograd.grad(loss, self.g1,
        ↪  create_graph=True)[0]
        dg2_loss = torch.autograd.grad(dg1_loss, self.g2,
        ↪  create_graph=True)[0]

        #return the loss
        return dg2_loss

########################## Implement the protocol
steps=0 #recomend to set it at 100
t=0.0
g=0.0
min_val_list =[]
min_val_parameters = []

nmin = 0
nmax = 0 #recomend to set it at (2,45) if you want to try the code

for N in range(nmin,nmax):
    #constants required for the vector
    B = np.flip(np.arange(N+1))
    vec_binom = torch.sqrt(torch.tensor(special.binom(N,B),dtype =
    ↪  torch.cfloat))

    #definition of the matrices
    Jx,Jy,Jz=H(N)
    Jxx=Jx@Jx
    Jyy=Jy@Jy

    #dimension of the system
    dim=N+1

    #machine learning implemented
    my_loss = LossFunction(Jxx,Jyy,Jz,dim,t,g,N)
    my_optimizer = optim.Adam(my_loss.parameters(), lr=0.001)

    #lists
    loss_list = []
    theta_vals_list = []

    #define figure to check how the protocol is doing
    fig = plt.figure()

    for i in range(steps):
        #loss function working
        for j in range(1000):

            #this is necessary to "reset" the gradients
            my_optimizer.zero_grad()
```

```
136
137             #Compute the value of the loss function in the current value
                ↪  of the theta parameters
138             loss = my_loss()
139
140             #Compute the gradients
141             loss.backward()
142
143             #perform one optimization step
144             my_optimizer.step()
145
146             #save the value of the loss function and of the theta
                ↪  parameters
147             loss_list.append([1000*i+j,loss.detach().numpy()])
148
                ↪  theta_vals_list.append(torch.clone(my_loss.theta_vec).detach().numpy())
149
150         arloss_list = np.array(loss_list)
151
152         #plot the quantum fisher info to see what is going on
153         fig.clear()
154         plt.plot(arloss_list[:,0],arloss_list[:,1])
155         plt.ylim(-101,1)
156
157         plt.show()
158         min_val = np.min(arloss_list[:,1])
159         print(min_val)
160         print("spin number",N)
161         clear_output(wait=True)
162         if min_val == min_val_pre:
163             break
164         min_val_pre = min_val
165
166     min_val_list.append(min_val)
167     theta_vals_list = np.array(theta_vals_list)
168     old=theta_vals_list[-1]
169
    ↪  min_val_parameters.append((theta_vals_list[np.argmin(arloss_list[:,1])]).tolist()
170
171
172
173
174
```